

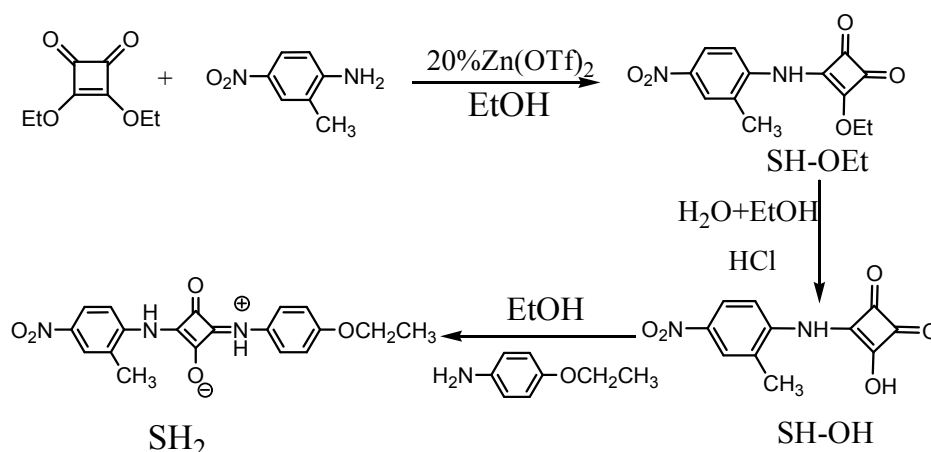
# A Squaraine-Based Colorimetric Chemosensor for Extremely Sensitive and Recyclable CO<sub>2</sub> Detection: Highly Off-On-Off response

Guomin Xia, Yang Liu, Benfei Ye, Jianqi Sun, Hongming Wang\*

## Experimental

### General

All starting chemicals and solvents were purchased from commercial suppliers and used as received unless explicitly stated. Absorption spectrometry was performed using Gold S54T spectrophotometer of Lengguang Company. Melting points were determined in open capillaries. <sup>1</sup>H NMR and <sup>13</sup>C NMR spectra were measured on a Bruker AVANCE 400 spectrometer in DMSO-d<sub>6</sub> using TMS as an internal standard. Elemental analysis was performed on Elementar Vario vario EL III. Mass spectra were acquired on Bruker maXis UHR-TOF. Tetrabutylammonium salts (F<sup>-</sup>, AcO<sup>-</sup>, Cl<sup>-</sup>, Br<sup>-</sup> and I<sup>-</sup>) were all >98% pure and the solutions used in titrations were prepared in fresh dry DMSO.



**Scheme S1.** The synthesis of receptor SH<sub>2</sub>

### Synthesis of Squarate Monoester (SH-OEt)

To a 25ml round bottom flask was added diethyl squarate (296μl, 2mmol), 2-methyl-4-nitroaniline (304mg, 2mmol) and zinc trifluoromethanesulfonate (Zn(OTf)<sub>2</sub> 146mg, 20mol%) in 20ml distilled ethanol. the reaction mixture was strongly stirred at 100°C for 2h and then filtered,

the obtained solid residue was washed with excess ethanol to give orange powder squarate monoester (SH-OEt) at the yield of 86% (475 mg, 1.72mmol).

### Synthesis of Semisquaraine (SH-OH)

To a 50ml round bottom flask was added squarate monoester (414mg, 1.5 mmol) and 1ml 3M HCl in an 20ml aqueous ethanol solution (volume 1:1). the mixture was refluxed for 2h at 100°C and then filtered, the obtained solid residue was washed with excess hot ethanol to give orange powder (SH-OH) at the yield of 83% (308mg, 1.24mmol), which was used in the next step without any further purification.

### Synthesis of Squaraine (SH<sub>2</sub>)

To a 50ml round bottom flask was added semisquaraine (248.5mg, 1mmol), Phenetidine (205mg, 1.5mmol) in 20ml distilled ethanol. After reflux for 10 h at 100°C, the mixture was filtered; the obtained solid residue was washed with excess hot ethanol to give orange powder SH<sub>2</sub> at the yield of 89% (326mg, 0.89mmol). M.P. >300°C. <sup>1</sup>H NMR (400 MHz, DMSO-d<sub>6</sub>) δ ppm 1.29 (t, *J* = 6.83 Hz, 3H), 2.44 (s, 3H), 3.99 (q, *J* = 6.64 Hz, 2H), 6.93 (d, *J* = 8.84 Hz, 2H), 7.63 (d, *J* = 8.75 Hz, 1H), 7.71 (d, *J* = 8.74 Hz, 2H), 8.07 (d, *J* = 8.95 Hz, 1H), 8.10 (s, 1H), 10.84 (s, 1H), 11.75 (s, 1H). <sup>13</sup>C NMR (400 MHz, DMSO-d<sub>6</sub>) δ ppm 180.19, 175.15, 156.58, 143.98, 142.08, 131.29, 131.07, 126.02, 122.24, 122.08, 115.31, 63.70, 1821. 15.05. Anal. Calcd for SH<sub>2</sub>: C, 62.12; H, 4.66; N, 11.44. Found: C, 62.10; H, 4.70; N, 11.46. ESI-MS: *m/z* =negative ions, [M-H]<sup>-</sup>=366.09.

Computational method.

All calculations were performed using the Gaussian 09 package<sup>1</sup>. Theoretical calculation for the geometrical optimization of receptor SH<sub>2</sub>, SH<sup>-</sup> and S<sup>2-</sup> was performed at the density functional theory (DFT) level using the B3LYP<sup>2</sup> and mpw1pw91<sup>3</sup> hybrid functional. The 6-311G(d,p) basis sets were employed all atoms. After obtaining the optimized structure, the further time-dependent density functional theory (TD-DFT) calculation was performed to investigate the excited states using the B3LYP method. For the reaction mechanism calculation, mpw1pw91 functional was used. All reactants and intermediate had no imaginary frequency, and the transition states were ascertained by vibrational analysis with only one imaginary frequency mode. The zero-point energy was calculated by using the vibrational frequencies. In the case of transition states, the vibration was associated with a movement in the direction of the reaction coordinate. Intrinsic reaction coordinate calculations, at the same level of theory, were performed to ensure that the transition states led to the expected reactants and products. The solvent effects have been considered using a relatively simple self-consistent reaction field (SCRF) method, based on the polarizable continuum model (PCM).<sup>4</sup> The solvent used in this calculation is DMF. The values of the relative energies with zero-point energy correction ( $\Delta E_0$ ) were calculated and used on the basis of the total energies of the stationary points.

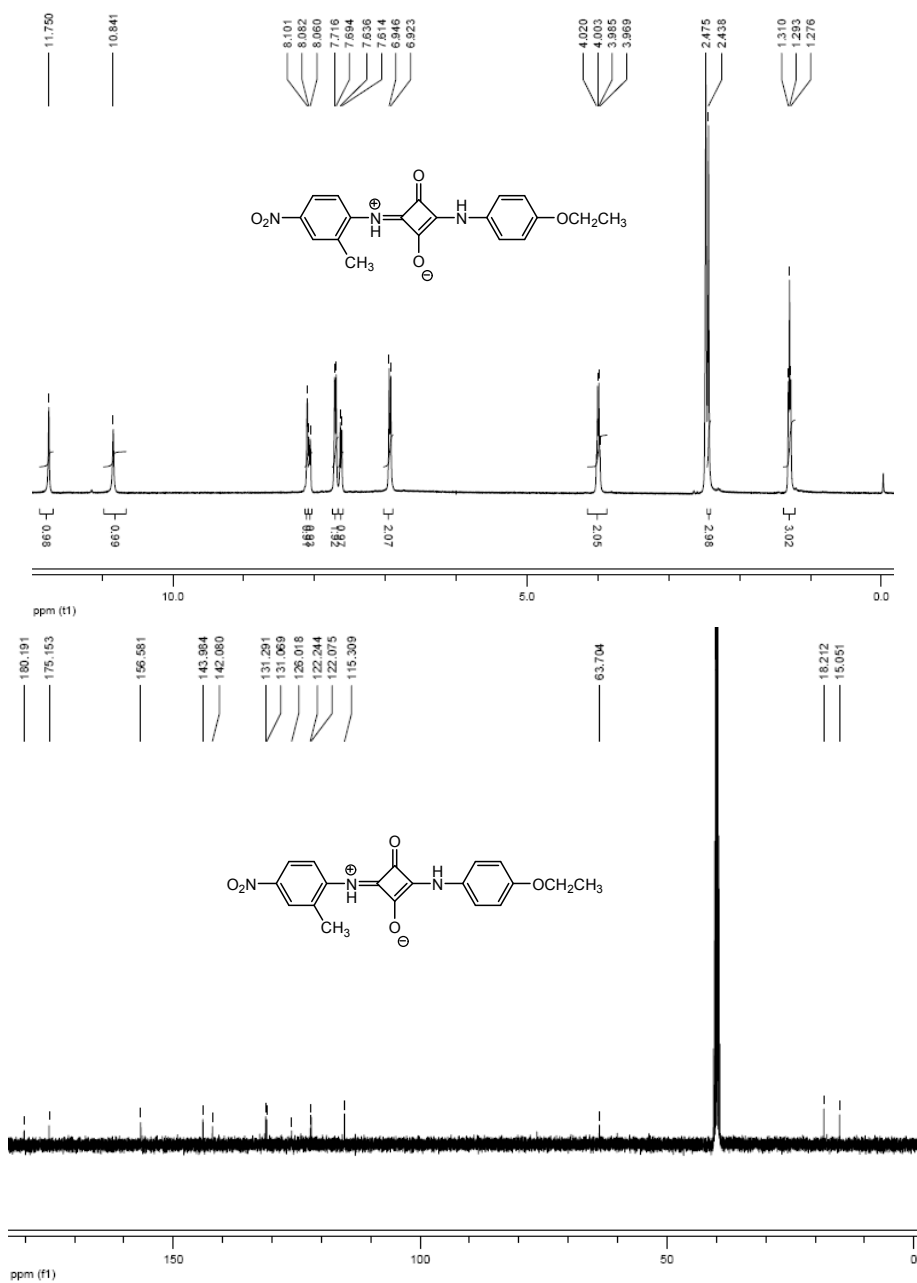


Figure S1. the <sup>1</sup>H NMR (addition of CF<sub>3</sub>COOH) and <sup>13</sup>C NMR record of SH<sub>2</sub> compound.

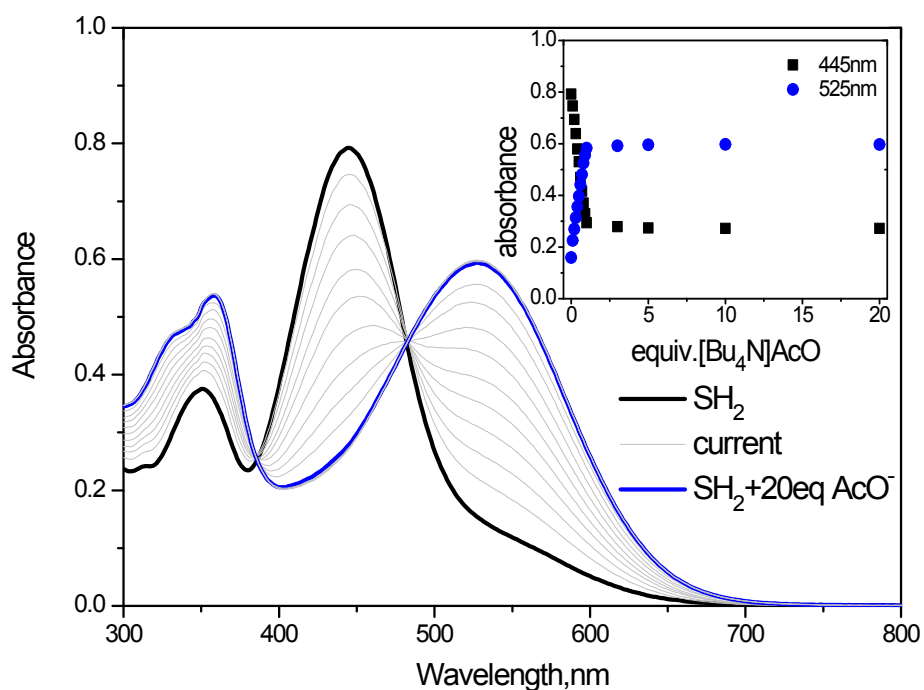


Figure S2. UV-vis spectra taken over the course of titration of receptor SH<sub>2</sub> (30 μM) with equivalent [Bu<sub>4</sub>N]AcO in DMSO. Inset: Their corresponding plots of absorbance at indicated wavelengths versus additional [Bu<sub>4</sub>N]AcO.

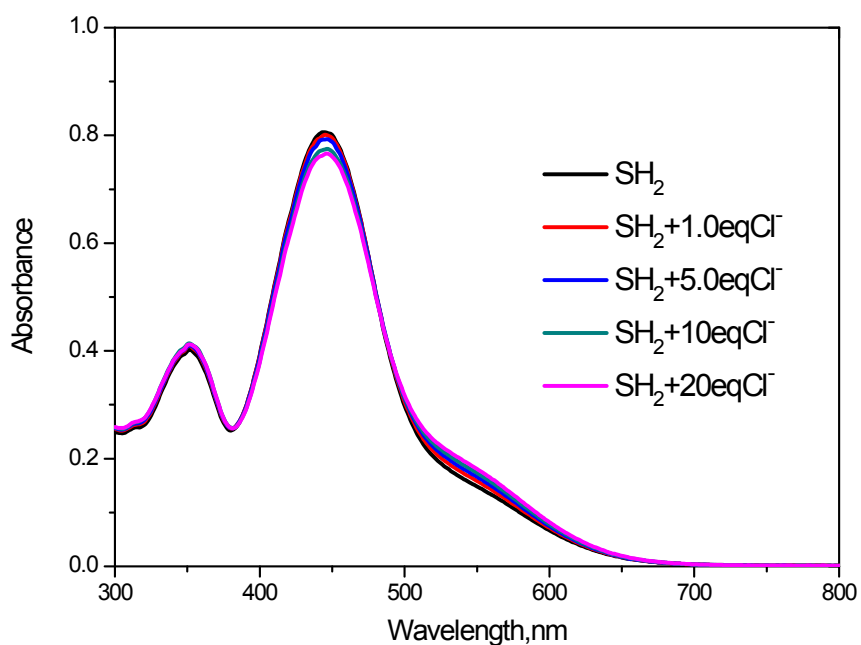


Figure S3. UV-vis spectra taken over the course of titration of receptor SH<sub>2</sub> with equivalent [Bu<sub>4</sub>N]Cl in DMSO.

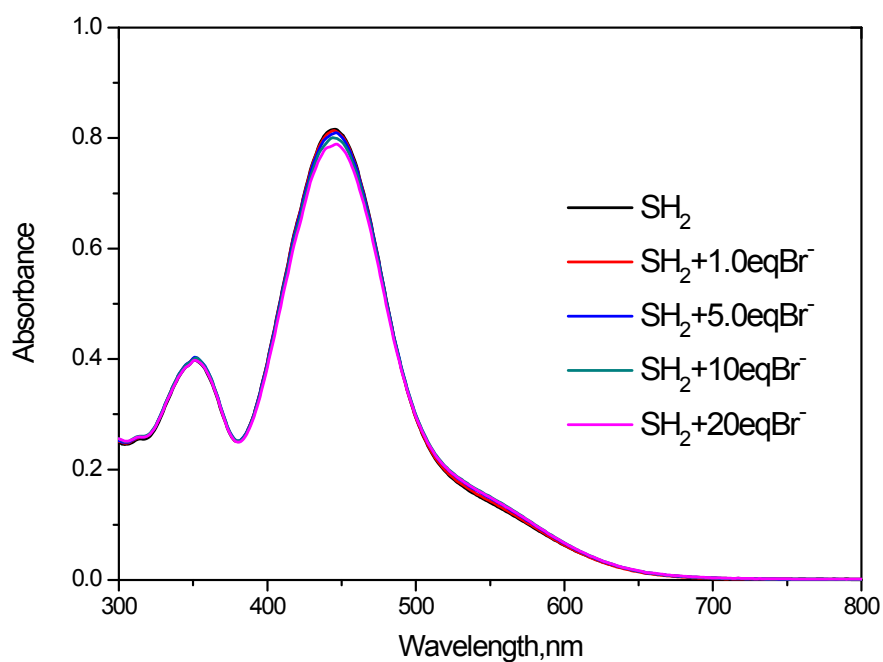


Figure S4. UV-vis spectra taken over the course of titration of receptor SH<sub>2</sub> (30 μM) with equivalent [Bu<sub>4</sub>N]Br in DMSO.

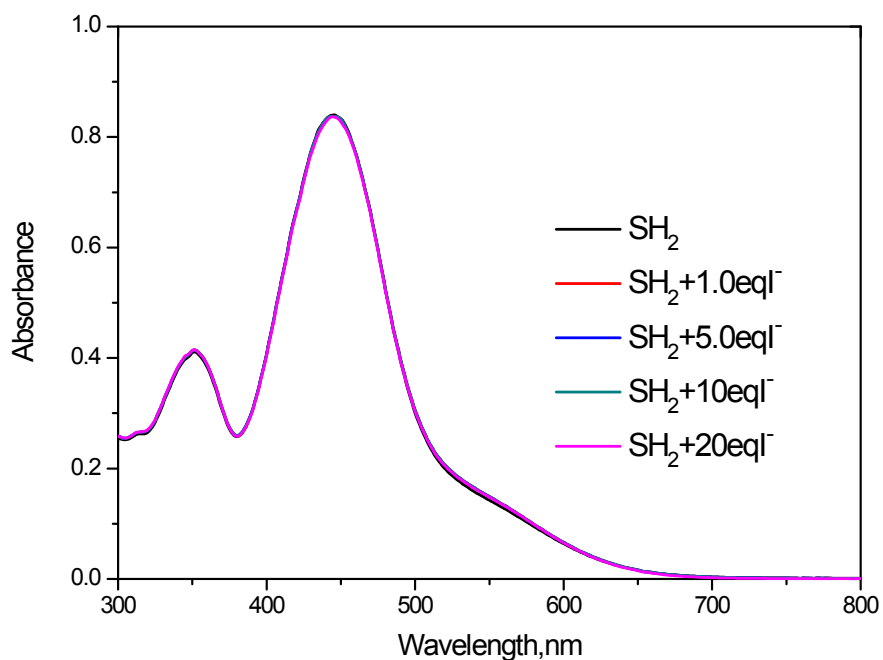


Figure S5. UV-vis spectra taken over the course of titration of receptor SH<sub>2</sub> (30 μM) with equivalent [Bu<sub>4</sub>N]I in DMSO.

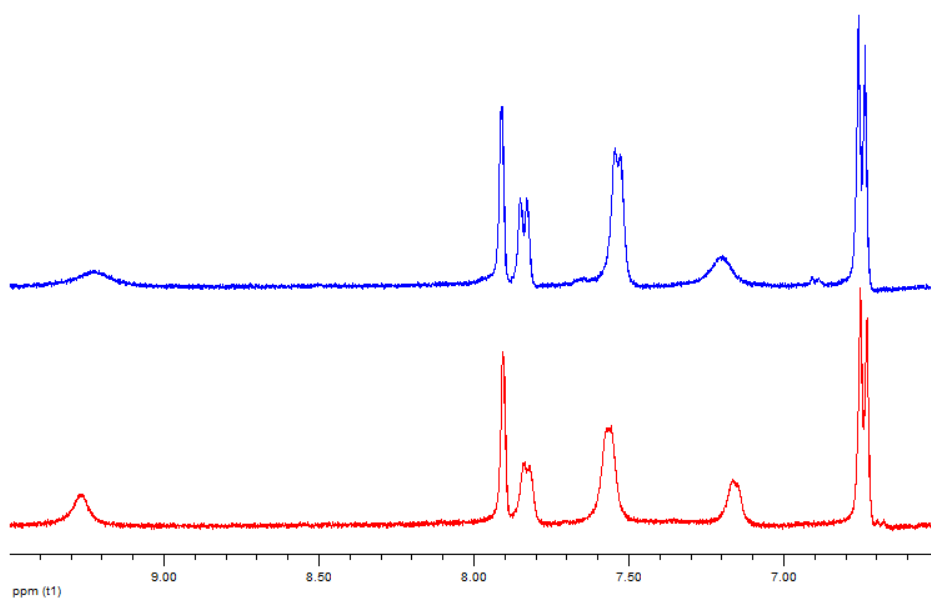


Figure S6. Comparing with adding sodium bicarbonate into the receptor  $\text{SH}_2$  solution after 5.0-fold  $\text{F}^-$  ions added (the red,  $\text{SH}_2 + 5\text{eq F}^- + \text{NaHCO}_3$ ; The blue,  $\text{SH}_2 + 5\text{eq F}^- + \text{CO}_2$ ).

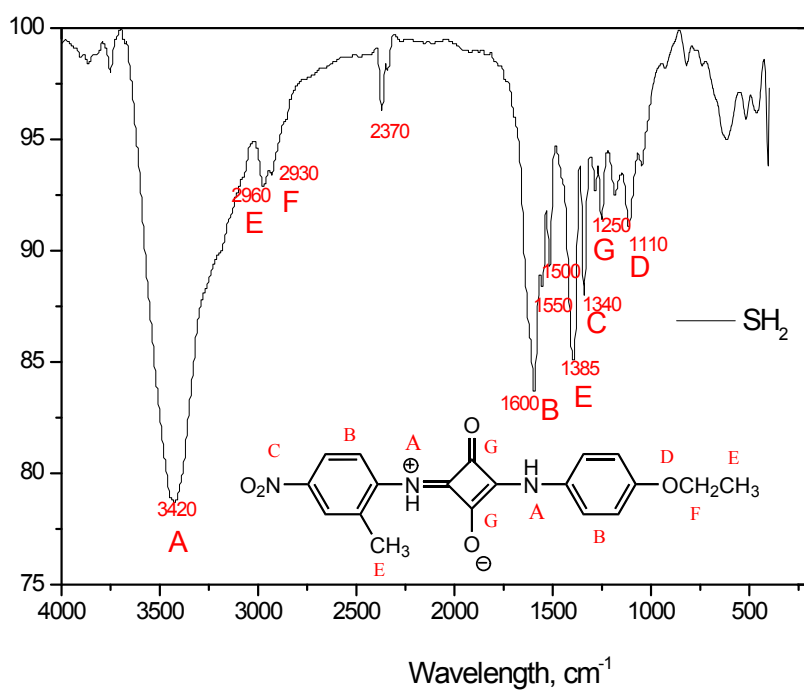


Figure S7. The IR spectrum of  $\text{SH}_2$ .

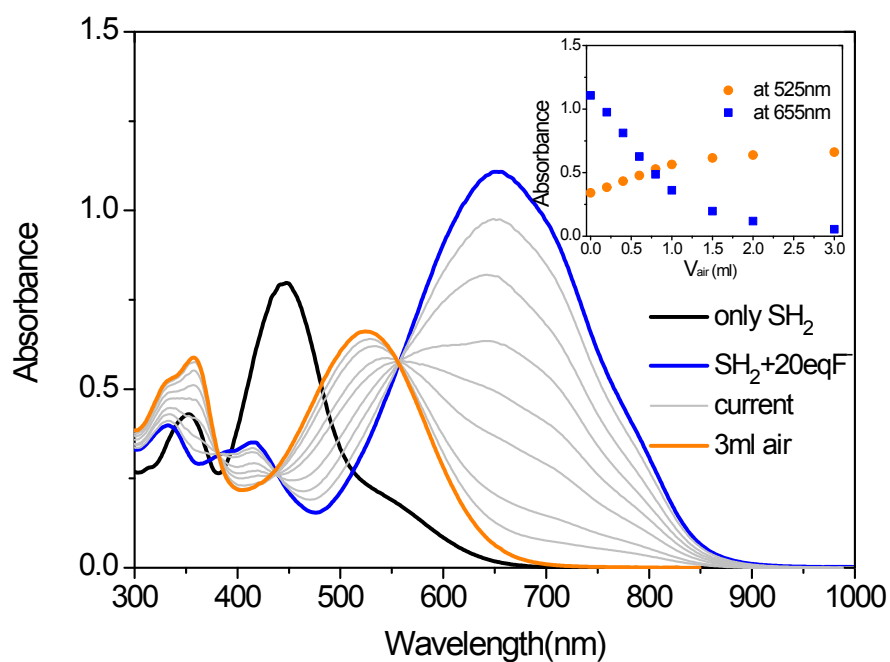


Figure S8. UV-vis spectra taken over the course of titration of receptor SH<sub>2</sub> (30 μM) with excess TBAF in DMSO then bubbling with different volumes of air gas in a sealed cuvette. Inset: Their corresponding plots of absorbance at indicated wavelengths versus additional volume of air gas.

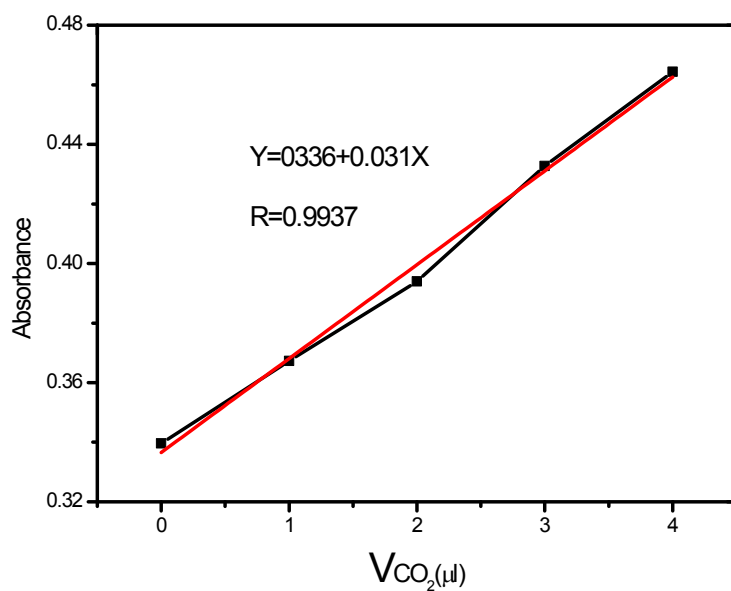


Figure S9. The absorbance of SH<sub>2</sub> at 525 nm versus the volume of CO<sub>2</sub> gas.

**Detection Limit** <sup>[5]</sup>. The detection limit was calculated on the basis of the UV-Vis titration. The UV-Vis spectrum of SH<sub>2</sub> treated with 20eq [Bu<sub>4</sub>N]F was measured 11 times, and the standard deviation of blank measurement was achieved. To gain the slope, the absorbance at 525 nm versus amount of CO<sub>2</sub> gas was plotted. The detection limit was calculated using the following equation:

$$\text{Detection limit} = 3\sigma/k \quad (1)$$

Where  $\sigma$  is the standard deviation of blank measurement, and  $k$  is the slope between the absorbance versus the volume of CO<sub>2</sub> gas ( $V_{\text{CO}_2}$ ).

The detection limit was calculated to be about  $0.64 \times 10^{-6} \text{M}$  (ca. 15.6 ppm).

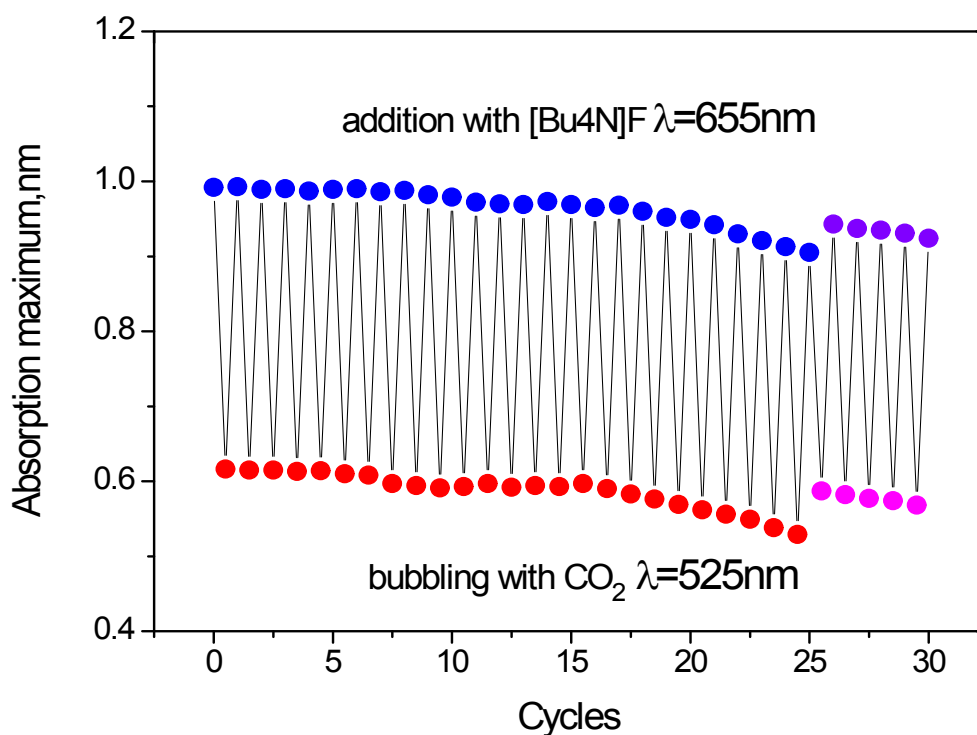


Figure S10. Reversible switching the absorption ( $\lambda_{\text{abs}}$ ) of receptor SH<sub>2</sub> (30  $\mu\text{M}$ ) by repeated addition of 4  $\mu\text{l}$  TBAF (0.45M, the blue), 12  $\mu\text{l}$  CO<sub>2</sub> gas (the red), 8  $\mu\text{l}$  TBAF (0.45M, the purple), 24  $\mu\text{l}$  CO<sub>2</sub> gas (the pink) in 3ml DMSO.



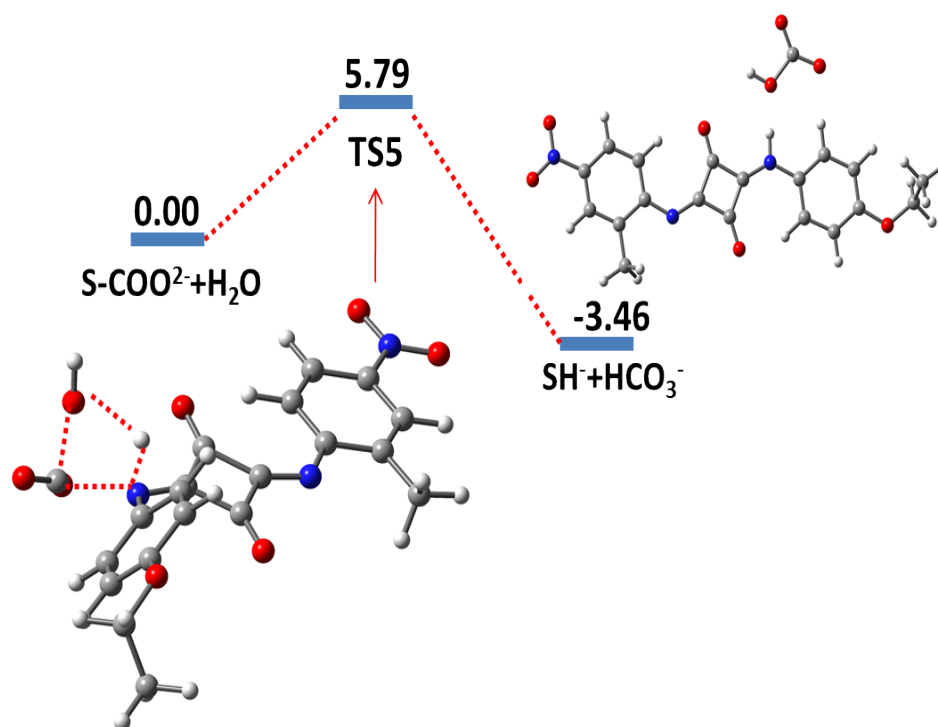


Figure S11. The reaction energy profile of S-CO<sub>2</sub><sup>2-</sup> with H<sub>2</sub>O (unit for energy: kcal mol<sup>-1</sup>).

Table S1. Selected data of electronic transitions in 1 by TD-DFT calculations using b3lyp/6-311g(d,p) method.

	$\lambda$ [nm/(eV)]	f	Composition of bands and CI coefficients
SH <sub>2</sub>	421.77nm (2.94eV)	f=0.4333	HOMO → LUMO 0.70343
SH <sup>-</sup>	539.13nm (2.13 eV)	f=0.9597	HOMO → LUMO 0.70832
S <sup>2-</sup>	616.9nm (2.01eV)	f=1.486	HOMO → LUMO 0.71131

#### References

- 1 M. J.Frisch, G. W.Trucks, H. B.Schlegel, G. E. Scuseria, M. A. Robb, J. R.Cheeseman, G. Scalmani, V. Barone, B.Mennucci, G. A.Petersson, H.Nakatsuji, M.Caricato, X.Li, H. P.Hratchian, A. F.Izmaylov, J.Bloino, G.Zheng, J. L.Sonnenberg, M.Hada, M.Ehara, K.Toyota, R.Fukuda, J.Hasegawa, M.Ishida, T.Nakajima, Y.Honda, O.Kitao, H.Nakai, T.Vreven, J. A. Jr.Montgomery, J. E. Peralta, F.Ogliaro, M.Bearpark, J.J.Heyd, E.Brothers, K. N.Kudin, V. N.Staroverov, R.Kobayashi, J.Normand, K.Raghavachari, A. Rendell, J. C.Burant, S. S.Iyengar, J.Tomasi, M.Cossi, N.Regga, J. M.Millam, M.Klene, J. E.Knox, J. B.Cross, V.Bakken, C.Adamo, J.Jaramillo, R.Gomperts, R. E.Stratmann, O.Yazyev, A. J.Austin, R.Cammi, C.Pomelli, J. W.Ochterski, R. L.Martin, K.Morokuma, V. G.Zakrzewski, G. A.Voth, P.Salvador, J. J.Dannenberg, S.Dapprich, A. D.Daniels, O.Farkas, J. B.Foresman, J. V.Ortiz, J.Cioslowski, and D. J.Fox, Gaussian, Inc., Wallingford CT, 2009.
- 2 (a) C. T.Lee, W. T.Yang, R. G.Parr, *Phys. Rev. B* 1988, 37, 785. (b) A. D.Becke, *J. Chem. Phys.* 1993, 98, 5648. (c) B.Miehlich, A. Savin, H.Stoll, H. Preuss, *Chem. Phys. Lett.* 1989, 157, 200.
- 3 C, Adamo. V, Barone. *J. Chem. Phys.*, 199, 8108, 664.
- 4 (a) M. Cossi, V. Barone, R. Cammi, J. Tomasi, *Chem. Phys.Lett.* 1996, 255, 327. (b) M. T. Cancas, V. Mennucci, J.Tomasi, *J.Chem. Phys.* 1997, 107, 3032. (c) V.Barone, M.Cossi, J.Tomasi, *J.Comput. Chem.* 1998, 19, 404.
- 5 S. Samanta, S. Goswami, N, Hoque, A. Ramesh,G, Das, *Chem. Commun.*, 2014, 50, 11833—11836.